J. Phys. B: At. Mol. Opt. Phys. **40** (2007) 1131–1139 doi:10.1088/0953-4075/40/6/004

Electron-impact excitation of neutral boron using the *R*-matrix with the pseudostates method

C P Ballance[1], D C Griffin[1], K A Berrington[2] and N R Badnell[3]

[1] Department of Physics, Rollins College, Winter Park, FL 32789, USA
[2] School of Science and Mathematics, Sheffield Hallam University, Sheffield, S1 1WB, UK
[3] Department of Physics, Strathclyde University, Glasgow G1 ONG, UK

Received 28 November 2006, in final form 21 January 2007
Published 5 March 2007
Online at stacks.iop.org/JPhysB/40/1131

Abstract

We have carried out a large *R*-matrix with pseudostates (RMPS) calculation of the electron-impact excitation of neutral boron. The RMPS method has been employed for the excitation/ionization of many light fusion related species, but primarily for one or two active electrons. The present 640-term close-coupling calculation included three distinct pseudostate expansions. This enabled us to both converge the *N*-electron structure for three active open-shell electrons and accurately represent the high Rydberg and target continuum states. The derived Maxwell-averaged effective collision strengths will be employed to model the spectral emission from boron, which is of importance to both current (TEXTOR) and future (ITER) magnetic fusion reactors. The full set of effective collision strengths is available at the Oak Ridge National Laboratory Controlled Fusion Atomic Data Center Web site.

1. Introduction

The boronization of the plasma exposed surfaces of tokamaks has proved to be an effective way to produce very pure fusion plasmas [1] and has been applied in tokamak experiments such as TEXTOR at Jülich and ASDEX at Garching. For progress to be made in understanding the erosion of low *Z* materials such as Be, B and C in the next generation of fusion experiments, transport modelling requires complete and accurate electron-impact excitation data along each of the aforementioned iosonuclear sequences. For beryllium, a complete set of non-perturbative calculations for all excitation and ionization rates from every ion stage has already been carried out [2, 3]. In this paper, we shall consider the electron-impact excitation of neutral boron. Although Be and C are considered to be the primary candidates for plasma-facing surfaces in ITER, boron is used as a dopant for carbon in order to reduce the level of carbon chemical erosion from tokamak surfaces [4].

The data currently employed for the modelling of neutral boron within the ADAS package are derived from plane-wave Born calculations [5]. However, this simple approximation does not include any distortion of the continuum electrons nor any coupling between the bound target

levels. In addition, previous RMPS calculations [6–8] have shown that the omission of the coupling of the target levels to the target continuum can lead to significantly inflated excitation cross sections above the ionization limit, and therefore subsequent Maxwell-averaged collision strengths. An earlier study involving only hydrogenic systems [7] revealed that agreement in effective collision strengths between *R*-matrix and RMPS calculations was only achieved at C^{5+}, thereby suggesting that RMPS calculations are required for the entire boron isonuclear sequence. The present work shall complement the earlier RMPS calculation of Badnell *et al* [6] for singly ionized boron, and extend and improve upon the existing structure and scattering calculations of Marchalant *et al* [8] for neutral boron.

RMPS calculations have scaled dramatically with respect to computational complexity over the last few years. For example, the electron-impact excitation of near neutral hydrogenic species [7] requires only a single sequence of $nl\,^2$L pseudostate terms, whereas helium-like systems at least double the size of the problem by involving both $1snl\,^{1,3}L$ [9] pseudostates. The progression to electron-impact excitation of neutral beryllium [3] demands *two* configuration sequences (2s*nl* and 2p*nl*), again involving both singlet and triplet terms, and a further doubling of the problem size. For all of the above pseudostate calculations, the maximum principal quantum number included was greater than or equal to 11 in order to provide the density of continuum pseudostates required to eliminate large unphysical oscillations in the cross sections above the ionization threshold

For boron, unlike previous RMPS studies concerning only one or two active electrons outside a closed core, the present work includes three distinct ($2s^2nl$, 2s2p*nl* and $2p^2nl$) configuration expansions, two of which involve both doublet and quartet terms; all of these are necessary in order to converge both the *N*-electron structure and the coupling of the bound states to the target continuum. The primary difficulties in the target structure and coupling to the target continuum for B arise from the $2s2p^2$ configuration. The orbitals in this configuration have been corrected here through configuration interaction with the 2s2p*nl* and $2p^2nl$ sequences. These same pseudostate expansions also provide for coupling of $2s2p^2$ configuration with the target continuum.

The remainder of this paper is structured as follows. In the next section we outline the RMPS method and discuss our model for neutral boron. In section 3, we compare our current findings with existing theoretical calculations, and finally in the last section, we summarize our present work and possible future directions.

2. Computational methods

The target radial wavefunctions employed in this calculation were generated using GASP (Graphical AutoStructure Package) [10]. This is a java-based front end to the atomic structure code AUTOSTRUCTURE [11]. GASP provides an efficient and intuitive method to define hundreds of *N*-electron configurations, each involving many orbitals. Spectroscopic orbitals were employed for those subshells from 1s to 4f and were determined from a local potential using Slater-type orbitals. A set of non-orthogonal Laguerre pseudo orbitals was then generated from 5s to 11g; they were subsequently orthogonalized to the spectroscopic orbitals and to each other. It was determined that three distinct pseudostate expansions gave the best representation of the *N*-electron target and provided a sufficient density of pseudostates from the ionization threshold to 20 eV. These *N*-electron target configurations are defined as follows:

- $2s^2nl$ $n = 2$–11 $l = 0$–4
- 2s2p*nl* $n = 2$–11 $l = 0$–4
- $2p^2nl$ $n = 2 - 11$ $l = 0$–3

We have omitted the $2p^2 8g$, $2p^2 9g$, $2p^2 10g$, $2p^2 11s$, $2p^2 11d$ and $2p^2 11g$ configurations as they have minimal influence on the structure of the first 11 terms. Our goal was to provide effective collision strengths for all transitions between the lowest 11 terms through the $2s^2 5s\ ^2S$ term. Configuration interaction with the higher $2s^2 ns$ pseudostates renders the $2s^2 5s$ term essentially spectroscopic in terms of both energy and radiative rates. In addition, the above three pseudostate sequences lead to excellent energies for these 11 terms and ensure that all important couplings of these terms to the high-Ryderg states and the target continuua are included. The resulting 640 terms were employed in both the configuration-interaction expansion of the target and in the close-coupling expansion. Although our theoretical target energies are very close to the experimental values (see section 3), due to future modelling applications of our work, they were shifted to the experimental values. Finally, AUTOSTRUCTURE was also used to generate the infinite energy Bethe/Born limits that permit interpolation of explicitly calculated RMPS results into higher temperature regimes.

In the RMPS method introduced by Bartschat *et al* [12], Sturmian orbitals were employed to represent the target continuum. In our RMPS implementation [13, 14], we use the pseudostate method described in [15]. The present calculation was performed with our set of parallel R-matrix codes that are extensively modified versions of the serial RMATRIX I codes [16]. The scattering calculation involved dividing the partial-wave angular momentum into three $LS\Pi$ ranges in order to minimize the size of the Hamiltonian matrices that were repeatedly diagonalized. For singlet, triplet and quintet symmetries with angular momentum in the range $L = 0$–9, 32 continuum basis orbitals were used to span the incident electron energy from 0 to 23 eV; for the range $L = 10$–20 a basis of 30 orbitals was employed and in the final angular momentum range from $L = 21$ to 40 only 22 basis orbitals were required. In the final angular momentum range, the two-electron exchange integrals were not included. This is consistent with the usual procedure of using the non-exchange codes [17] for partial-wave symmetries with angular momentum $L > 12$. The R-matrix radius was set at 70.0 Bohr radii and with over 1700 scattering channels for certain partial waves, the calculation produced large Hamiltonian matrices up to 60 000 by 60 000 in size. Using the parallel suite of R-matrix codes, all partial waves in each range were calculated simultaneously, and we note that those symmetries involving up to six to seven thousand $(N + 1)$-electron bound terms did not take significantly longer than those involving the largest number of scattering channels. For each partial wave, there are (n channels $*$ (n channels+1)/2) continuum–continuum blocks for a particular $(N + 1)$-electron Hamiltonian matrix, and as the number of channels increases, it is the formation of these blocks that begins to dominate the computational time for the inner-region portion of the calculation. Due to the relatively small energy separation between the first excitation threshold of 0.263 Ryd and the ionization threshold of 0.61 Ryd, only 400 incident-electron energy mesh points were required from 0.263-0.663 Ryd to map out these slowly varying cross sections. In the energy range above the ionization threshold, we have restricted our calculation to incident-electron energies from 0.7 Ryd to 1.5 Ryd. The maximum energy chosen is justified by the ionization balance calculations of Mazzota *et al* [18], which show that the ionic fraction of neutral boron is negligible beyond a temperature of 6×10^4 K.

The contributions from the higher angular momentum ($L > 40$) were estimated as follows: the dipole transitions were topped-up using a method originally described by Burgess [19]; the non-dipole transitions were topped-up assuming a geometric series in L, using energy ratios, and with a special procedure to handle transitions between nearly degenerate levels based on the degenerate limiting case [20]. Any method that represents the target continuum by a finite set of L^2 basis functions will exhibit a degree of oscillation in the cross section above the ionization threshold. We consider the calculation to be converged when these oscillations

Table 1. Energies of the first 11 terms of B I relative to the $(2s^2 2p)^2P$ ground state. All energies are in Rydbergs. Experimental values refer to the NIST database, but based upon the experimental work of Odintzova and Strignov. The theoretical results are from [21] and [25].

No.	Configuration	Term	Energy present	Energy theory [25]	Energy theory [21]	Energy experiment
1	$2s^2 2p$	^2p	0.000	0.000	0.000	0.000
2	$2s2p^2$	^4P	0.261	0.256	–	0.263
3	$2s^2 3s$	^2S	0.367	0.372	0.365	0.365
4	$2s2p^2$	^2D	0.441	0.448	–	0.436
5	$2s^2 3p$	^2P	0.442	0.461	–	0.443
6	$2s^2 3d$	^2D	0.499	0.517	0.499	0.499
7	$2s^2 4s$	^2S	0.501	–	0.501	0.501
8	$2s^2 4p$	^2P	0.525	–	–	0.527
9	$2s^2 4d$	^2D	0.545	–	0.547	0.547
10	$2s^2 4f$	^2F	0.545	–	–	0.547
11	$2s^2 5s$	^2S	0.549	–	0.548	0.548

Table 2. Oscillator strengths from the ground state and $(2s^2 3p)^2P$ term. The present work is compared with the theoretical values of Marchalant *et al*.

Transition	Present (length)	Ratio (l/v)	Marchalant *et al* (length)	Marchalant *et al* ratio (l/v)
$(2s^2 2p)^2P \rightarrow (2s^2 3s)^2S$	0.073 34	0.99	0.079 72	1.02
$(2s^2 2p)^2P \rightarrow (2s^2 3d)^2D$	0.016 48	1.02	0.178 70	1.16
$(2s^2 2p)^2P \rightarrow (2s^2 4s)^2S$	0.012 45	1.05	–	–
$(2s^2 2p)^2P \rightarrow (2s^2 4d)^2D$	0.072 40	1.05	–	–
$(2s^2 3p)^2P \rightarrow (2s^2 3s)^2S$	1.073 00	1.02	1.212 10	1.27
$(2s^2 3p)^2P \rightarrow (2s^2 3d)^2D$	0.852 59	0.99	0.877 60	1.03
$(2s^2 3p)^2P \rightarrow (2s^2 4s)^2S$	0.192 22	1.04	–	–
$(2s^2 3p)^2P \rightarrow (2s^2 4d)^2D$	0.000 48	0.78	–	–

are sufficiently small that they have no appreciable impact on the Maxwell-averaged effective collision strengths.

3. Results

In table 1, we compare our present target energies with the elaborate MQDT theory calculations of Liang and Wang [21] for the $2s^2 ns$, nd sequences and the experimental values of Odintzova and Striganov [22], reported in the NIST database [23]. We also note that the theoretical energy levels presented in [24] were transcribed incorrectly; however, subsequent correspondence with one of the authors [25] has provided the amended values given in table 1. The current calculation clearly provides improved energies over the target structure employed in this most recent RMPS scattering calculation. The average difference between our calculated energies and the experimental values [22] is 0.35%. The remaining differences could be minimized further with the inclusion of additional pseudostates with higher principal quantum numbers; however, the slight additional improvements in the target structure that would be achieved are far outweighed by the computational cost of an even larger scattering calculation.

In table 2, we present a selection of the strongest dipole-allowed oscillator strengths from the ground state and the $(2s^2 3p)^2P$ excited term; we note the almost unitary length to velocity

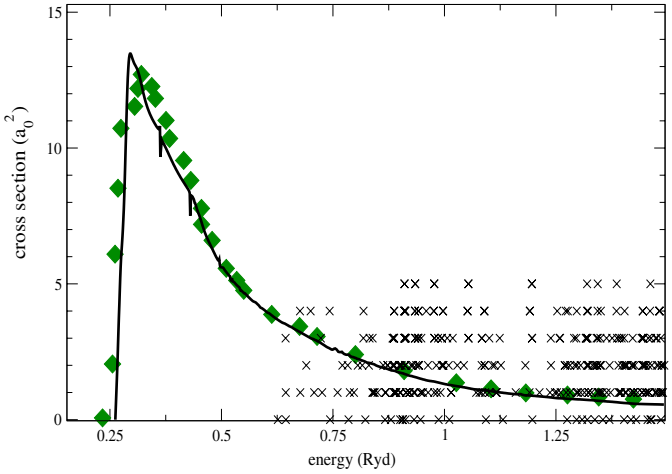

Figure 1. Cross section for the $(2s^2 2p)^2P$ to $(2s2p^2)^4P$ transition, in units of a_0^2. Diamonds: Marchalant *et al* [8]; solid: present calculation. The crosses represent the distribution of pseudostates above the ionization threshold, with the y axis defining the angular momentum of the individual pseudostate terms.

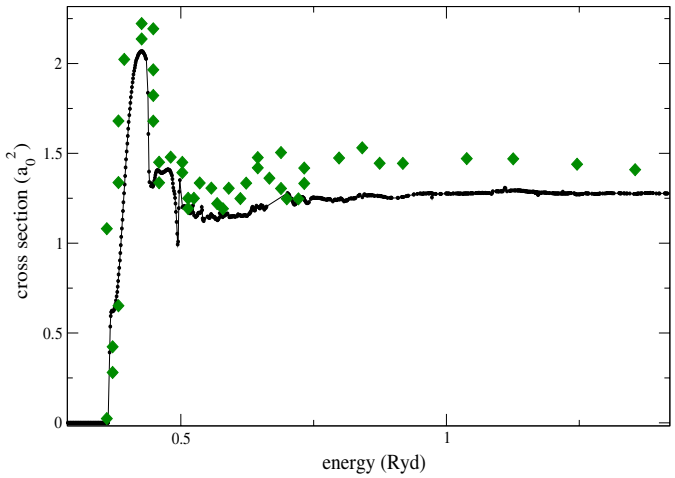

Figure 2. Cross section of the $(2s^2 2p)^2P$ to $(2s^2 3s)^2S$ transition, in units of a_0^2. Diamonds: Marchalant *et al* [24]; solid: present calculation.

ratios of the present calculation. They are improved over the oscillator strength length to velocity ratios for the $n = 3$ terms obtained by Marchalant *et al* [8], which are also given in this table. For transitions involving the $n = 4$ terms, only the weak $(2s^2 3p)^2P \rightarrow (2s^2 4d)^2D$ transition has a length to velocity ratio appreciably different from 1.0. The radiative rates available in the NIST database [23] are not included in this comparison as they are classified with an accuracy rating of C or less.

There are 55 possible transitions amongst the first 11 spectroscopic terms; the six transitions discussed below provide a representative sample of these excitations. Figure 1 was chosen in order to show the level of agreement between the present calculation and the previous RMPS calculation for transitions between $n = 2$ terms. Figures 2 and 3 highlight

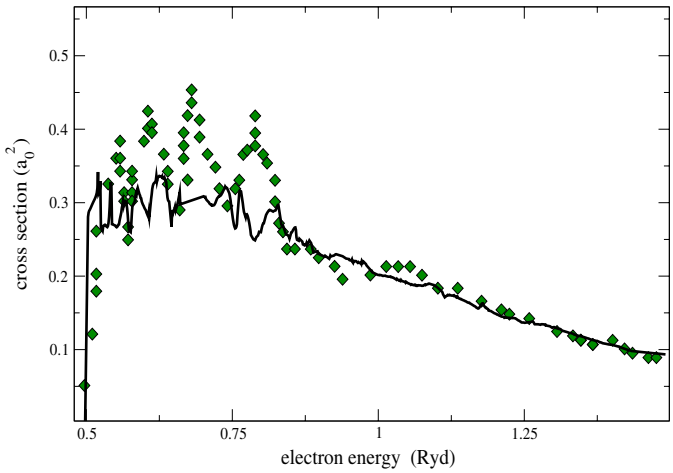

Figure 3. Cross section of the $(2s2p^2)^4P$ to $(2s^23d)^2D$ transition, in units of a_O^2. Diamonds: Marchalant *et al* [24]; solid: present calculation.

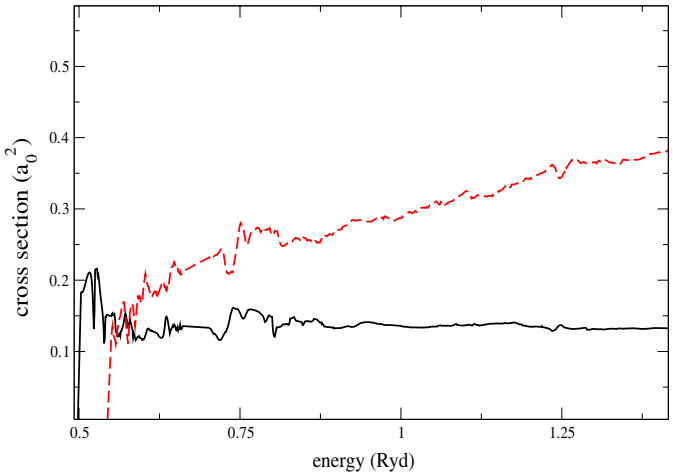

Figure 4. Cross section for excitation from $(2s^22p)^2P$ to both the $(2s^24s)^2S$ and $(2s^24d)^2D$ terms in units of a_O^2. solid: 4s; dashed: 4d.

the improved convergence of our calculations over the previous work for transitions to the $n = 3$ terms from the ground and metastable terms. In figure 4, we show transitions involving the $n = 4$ terms that have not been included in the earlier RMPS calculation. Finally in figure 5, we consider a near-degenerate dipole transition, which is insensitive to the effects of continuum coupling.

As illustrated in figure 1, there is excellent agreement with the earlier RMPS calculation for the transition from the ground state to the $(2s2p^2)^4P$ term. This spin-forbidden transition has the largest peak cross section in the low energy region, and should strongly populate the metastable term at low temperatures. It is only beyond 0.5 Ryd that the ground state to the $(2s2p^2)^2D$ cross section begins to have a comparable magnitude. Also incorporated within figure 1 is the energy distribution of those pseudostates that are above the ionization threshold,

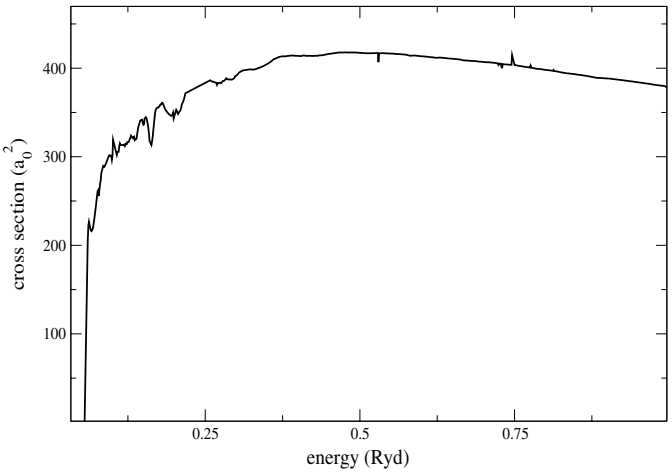

Figure 5. Cross section of the near degenerate dipole allowed the $(2s^2 3p)^2P$–$(2s^2 3d)^2D$ transition in units of a_O^2.

grouped according to their term angular momentum. A significant number of pseudostates lie above 20 eV, but as explained previously [18], we have not pursued scattering calculations in this energy range.

Figure 2 shows the electron-impact excitation cross section for the dipole-allowed transition $(2s^2 2p)^2P$–$(2s^2 3s)^2S$. Above the ionization threshold the almost flat cross section obtained from the present calculation does not exhibit any of the pseudoresonances evident in the earlier RMPS calculation [24]; this clearly illustrates the high level of convergence of the present pseudostate expansion.

In figure 3, we show the two-electron excitation from the metastable $(2s2p^2)^4P$ to the $(2s^2 3d)^2D$ term. At energies above approximately twice the ionization threshold, there is excellent agreement with results from the earlier RMPS results [24]. However, in the low-energy region, the pseudoresonances that straddle the ionization threshold in the earlier work are probably due to a lack of convergence in the 2s2pnl expansion. Large unphysical resonances like those close to an excitation threshold have a large impact on low temperature effective collision strengths. We note that in order to make this comparison, we had to shift the energy scale used in figure 3 of [24] so that it is relative to the ^4P metastable term, rather than the ground state.

The RMPS cross sections for transitions from the ground state to higher n shells in neutral atomic systems will exhibit more pseudoresonance structure as the magnitude of the background cross section weakens. It has been shown in the previous work on helium [9] and beryllium [3] that for excitations from the ground state to high n shells close to the ionization theshold, there are differences of a factor of 2 or more between RMPS and standard R-matrix cross sections due to coupling to the target continuum. In figure 4, we show the cross sections for the dipole-allowed transitions from the ground state to the higher $(2s^2 4s)^2S$ and $(2s^2 4d)^2D$ terms. We would expect standard R-matrix calculations for boron to overestimate the cross section by a similar magnitude; therefore, the small undulations at 0.75 Ryd in our present calculation are acceptable in light of the large correction obtained from the use of these pseudostates to represent the continuum coupling.

In figure 5, we show the cross section for the strong dipole excitation $(2s^2 3p)^2P$–$(2s^2 3d)^2D$. The low angular momentum partial waves couple both of these terms to the target

continuum; however, because of the small excitation energy, the cross section for this transition is dominated by contributions from partial waves with high angular momentum. Thus the effects of continuum coupling for such excitations are quite small (see [26]). Above the energy for ionization from the $(2s^2 3p)^2P$ term of 0.167 Ryd, there are some small oscillations and a few small isolated spikes; however, for such a large cross section their effect on the Maxwell-averaged effective collision strengths is completely negligible.

We can conclude from these representative figures that, in comparison to earlier RMPS studies [8, 24], this calculation benefits significantly from the approximately 600 pseudostates that have been included above the ionization threshold. Cross sections involving transitions from the ground state to the $n = 2$ and $n = 3$ terms are much more fully converged, and we also expect highly accurate results for excitation to the $n = 4$ terms.

The full set of results for energy levels, dipole radiative rates and effective collision strengths (including Born/Bethe limits) for the first 10 terms over $T = 1 \times 10^4$–2×10^5 K, tabulated in the ADAS *adf04* format (Summers 1999) [27], is available via the WWW at http://www-cfadc.phy.ornl.gov/data_and_codes.

4. Summary

Highly accurate atomic structure and electron-impact excitation calculations for neutral boron have been made, which both improve and extend past work. The large pseudostate expansion brings both the target and scattering calculation to a higher levels of convergence than previously obtained.

Excitation rates for all ionization stages of boron are required in order to generate the generalized collisional radiative (GCR) coefficients [28] needed for the modelling of a plasma containing boron. With this calculation for the neutral species, RMPS results for electron-impact excitation are now available for every ionization stage. Results for B^+ [6] and B^{4+} [7] have been published previously. The unpublished results for B^{2+} and B^{3+} are now available. For B^{3+} the calculation follows the outline given in [29] and the B^{2+} calculation is similar to that used for He-like Be given in [3]. All these RMPS results will be archived in the form of Maxwell-averaged effective collision strengths both at Oak Ridge [30] and within the ADAS package [27].

Although we have considered only electron-impact excitation here, a similar calculation will also enable us to determine highly accurate ionization cross sections from the ground and metastable states of boron. Only the $2s^2nl$ and $2s2pnl$ sequences would be required for ground state ionization, whereas the metastable $(2s2p^2)^4P$ ionization also requires the $2p^2nl$ sequence. This will be considered in future work.

Acknowledgments

This research was partially supported by US DoE grant (DE-FG02-01ER54633) through Auburn University and a US DoE grant (DE-FG02-99ER54367) to Rollins College. Computational work was carried out at the National Energy Research Scientific Computing Center in Oakland, California and at the National Center for Computational Sciences in Oak Ridge, Tennessee. CPB and DCG would like to recognize the contribution of the summer undergraduate research program at Rollins College, and in particular, the efforts of Ms Jeanmarie Loria and Mr Erich Blossey in developing the GASP package. CPB would also like to acknowledge the application G3DATA written by Carl Frantz that was used in the preparation of this document.

References

[1] Winter J, Grobusch L, Rose T, Seggern J von, Esser H G and Wienhold P 1992 *Plasma Sources Sci. Technol.* **1** 82
[2] Colgan J, Loch S D, Pindzola M S, Ballance C P and Griffin D C 2003 *Phys. Rev.* A **68** 032712
[3] Ballance C P, Griffin D C, Colgan J, Loch S D and Pindzola M S 2003 *Phys. Rev.* A **68** 062705
[4] Davis J W and Haasz A A 1997 *J. Nucl. Mater.* **241–243** 37
[5] O'Mullane 2006 Private communication
[6] Badnell N R, Griffin D C and Mitnik D M 2003 *J. Phys. B: At. Mol. Opt. Phys.* **36** 1337
[7] Ballance C P, Badnell N R and Smyth E 2003 *J. Phys. B: At. Mol. Opt. Phys.* **36** 3707
[8] Marchalant P J, Bartschat K, Berrington K A and Nakazaki S 1997 *J. Phys. B: At. Mol. Opt. Phys.* **30** L279
[9] Ballance C P, Griffin D C, Badnell N R, Loch S D and Pindzola M S 2004 *Atomic Process in Plasmas 14th APS Topical Conference on Atomic Processes in Plasmas* ed J S Cohen, S Mazevet and D P Kilcreases, p 25 ISBN 0-7354-0211-6
[10] http://vanadium.rollins.edu/GASP.html
[11] Badnell N R 1997 *J. Phys. B: At. Mol. Opt. Phys.* **30** 1
[12] Bartschat K, Hudson E T, Scott M P, Burke P G and Burke V M 1996 *J. Phys. B: At. Mol. Opt. Phys.* **29** 115
[13] Mitnik D M, Griffin D C, Ballance C P and Badnell N R 2003 *J. Phys. B: At. Mol. Opt. Phys.* **36** 717
[14] Ballance C P and Griffin D C 2004 *J. Phys. B: At. Mol. Opt. Phys.* **37** 2943
[15] Gorczyca T W and Badnell N R 1997 *J. Phys. B: At. Mol. Opt. Phys.* **30** 2011
[16] Berrington K A, Eissner W B and Norrington P H 1995 *Comput. Phys. Commun.* **92** 290
[17] V M, Burke P G and Scott N S 1992 *Comput. Phys. Commun.* **69** 76
[18] Mazzotta P, Mazzitelli G, Colafrancesco S and Vittorio N 1998 *Astron. Astrophys. Suppl. Ser.* **133** 403
[19] Burgess A 1970 *J. Phys. B: At. Mol. Opt. Phys.* **7** L364
[20] Burgess A, Hummer D G and Tully J A 1974 *Phil. Trans. R. Soc.* A **266** 225
[21] Liang L and Wang Y C 2003 *J. Phys. B: At. Mol. Opt. Phys.* **36** 4387
[22] Odintzova G A and Striganov A R 1979 *J. Phys. Chem. Ref. Data* **8** 63
[23] http://physics.nist.gov
[24] Marchalant P J and Bartschat K 1997 *J. Phys. B: At. Mol. Opt. Phys.* **30** 4373
[25] Bartschat K 2006 Private communication
[26] Ballance C P, Griffin D C, Loch S D, Bovin R F and Pindzola M S 2006 *Phys. Rev.* A **74** 012719
[27] Summers H P 2005 *ADAS User Manual Version 2.9* webpage http://adas.phys.strath.ac.uk
[28] Summers H P, Dickson W J, OMullane M G, Badnell N R, Whiteford A D, Brooks D H, Lang J, Loch S D and Griffin D C 2005 *Plasma Phys. Control. Fusion* **48** 263
[29] Griffin D C, Badnell N R and Pindzola M S 1999 *J. Phys. B: At. Mol. Opt. Phys.* **32** L479
[30] http://www-cfadc.phy.ornl.gov/data_and_codes